University of Reading

Re-examining historical trends of tropical cyclone frequency

Article

Published Version

Creative Commons: Attribution 4.0 (CC-BY)

Open Access

Jones, K. R., Zhuo, J.-Y., Camargo, S. J., Hodges, K. I. ORCID: https://orcid.org/0000-0003-0894-229X, Bell, S. S. and Chand, S. S. (2026) Re-examining historical trends of tropical cyclone frequency. Geophysical Research Letters, 53 (14). e2026GL122083. ISSN 1944-8007 doi: 10.1029/2026GL122083 Available at https://centaur.reading.ac.uk/128267/

It is advisable to refer to the publisher's version if you intend to cite from the work. See Guidance on citing.

To link to this article DOI: http://dx.doi.org/10.1029/2026GL122083

Publisher: American Geophysical Union

All outputs in CentAUR are protected by Intellectual Property Rights law, including copyright law. Copyright and IPR is retained by the creators or other copyright holders. Terms and conditions for use of this material are defined in the End User Agreement.

www.reading.ac.uk/centaur

University of Reading

CentAUR

Central Archive at the University of Reading

Reading's research outputs online

Check for updates

Geophysical Research Letters

RESEARCH LETTER
10.1029/2026GL122083

Re-Examining Historical Trends of Tropical Cyclone Frequency

Kailey R. Jones[1,2], Jing-Yi Zhuo[1,3], Suzana J. Camargo[1,4], Kevin I. Hodges[5], Samuel S. Bell[6], and Savin S. Chand[6]

[1]Lamont-Doherty Earth Observatory, Columbia University, Palisades, NY, USA, [2]Now at: Department of Earth, Atmospheric, and Planetary Sciences, Purdue University, Purdue, IN, USA, [3]Now at: High Meadows Environmental Institute, Princeton University, Princeton, NJ, USA, [4]Columbia Climate School, Columbia University, New York, NY, USA, [5]National Centre for Atmospheric Science and Department of Meteorology, University of Reading, Reading, UK, [6]Institute of Innovation, Science and Sustainability, Federation University, Ballarat, VIC, Australia

Key Points:

- Tropical cyclone frequency trends in the 20th Century Reanalysis version 3 (20CRv3) vary with lifetime maximum wind intensity thresholds
- There is discontinuity in the tropical cyclone frequency time series from 20CRv3 linked with observational data changes
- Environmental discrepancies between 20CR versions since the pre-industrial era undermine confidence in reanalysis-based TC trend estimates

Supporting Information:

Supporting Information may be found in the online version of this article.

Correspondence to:

J.-Y. Zhuo,
jzhuo@princeton.edu

Citation:

Jones, K. R., Zhuo, J.-Y., Camargo, S. J., Hodges, K. I., Bell, S. S., & Chand, S. S. (2026). Re-examining historical trends of tropical cyclone frequency. *Geophysical Research Letters*, *53*, e2026GL122083. https://doi.org/10.1029/2026GL122083

Received 27 JAN 2026
Accepted 29 JUN 2026

Abstract The short duration of high-quality, reliable tropical cyclone (TC) observations limits our ability to detect long-term trends. Here, we analyze TC frequency trends in the NOAA 20th Century Reanalysis (20CR) versions 3 and 2c over the 19th and 20th centuries. TC counts in these data sets are particularly sensitive to TC lifetime maximum wind intensity thresholds, even with the sign of the trends reversed. Higher thresholds identify more organized vortex circulations and reveal observational inconsistencies inherited from assimilated sea-level-pressure data. Similar analysis is performed in other reanalysis data sets and tracking algorithms to assess the robustness of our results. Changes in large-scale environmental fields influencing TC activity since the pre-industrial era differ markedly between 20CR versions 3 and 2c, further reducing confidence in reanalysis-based trend assessments. Our results underscore the continuing challenge of inferring robust, long-term TC frequency changes from historical reanalyses.

Plain Language Summary Reliable observational records of tropical cyclones (TCs) are limited before the satellite era (post-1980s), making it difficult to assess long-term changes in TC activity. We examined TC frequency trends in two versions of the NOAA 20th Century Reanalysis spanning the full 20th century, and most of the 19th century. The impact of assimilating observed surface pressure from TC best-track data sets is clearly notable in the TC frequency time series. We performed a similar analysis using different reanalysis data sets, as well as with different tracking algorithms used to identify TCs to determine the robustness of our results. We also evaluated the changes in environmental variables that influence TC frequency, and found major discrepancy between the two versions of 20CR reanalysis, leading to the conclusion that these reanalysis products may not be suitable for determining reliable long-term TC frequency trends.

1. Introduction

Detecting and understanding how tropical cyclones (TCs) respond to anthropogenic climate change is crucial given their significant societal impacts. Has there already been a century-scale change in the global and regional TC counts associated with the current levels of global warming? The answer remains uncertain, largely owing to the relatively short and uneven observational record of TCs, which constrains reliable detection of long-term changes in TC activity (Camargo et al., 2023; Klotzbach et al., 2022; Knutson et al., 2019; Kossin et al., 2013).

Before the satellite era, global best-track records of TCs were especially prone to discontinuities and sampling gaps (Landsea, 2007; Landsea et al., 2010). Observations improved substantially with the advent of global satellite monitoring in the 1970s (Kossin et al., 2007), but the improved detection capability introduced a spurious upward trend in TC numbers by capturing storms that would previously have gone unrecorded (Landsea et al., 2010; Klotzbach et al., 2022). However, relying solely on the relatively short span of high-quality TC data hinders consensus on attribution to greenhouse warming, as short records likely contain substantial contributions from internal climate variation or non-greenhouse gas forcings (Knutson et al., 2019; Murakami et al., 2020; Vecchi et al., 2021).

Long-term reanalyses provide alternative data sets to assess trends in TC frequency extending back to the mid-19th century (e.g., Chand et al., 2022). These data sets combine historical observations with weather forecast models to produce a best-guess reconstruction of past atmospheric conditions, partially overcoming the limited

© 2026. The Author(s).
This is an open access article under the terms of the Creative Commons Attribution License, which permits use, distribution and reproduction in any medium, provided the original work is properly cited.

19448007, 2026, 14, Downloaded from https://agupubs.onlinelibrary.wiley.com/doi/10.1029/2026GL122083 by NICE, National Institute for Health and Care Excellence, Wiley Online Library on [16/07/2026]. See the Terms and Conditions (https://onlinelibrary.wiley.com/terms-and-conditions) on Wiley Online Library for rules of use; OA articles are governed by the applicable Creative Commons License

temporal and spatial coverage of direct observations (e.g., Slivinski, 2018). Using the NOAA (National Oceanic and Atmospheric Administration) 20th Century Reanalysis version 2c (20CRv2c), Chand et al. (2022) reported a robust declining trend in TC frequency at global and regional scales throughout the 20th Century. This finding has been challenged by Emanuel (2024), who argued that the apparent decline was an artifact of the increasing density of surface-pressure observations during the considered time period. He contended that observations assimilated into the model serves to both improve detection of real TCs and suppress model-generated storms, based on his analysis of the newer version 3 (20CRv3) data set. Chand et al. (2023) responded to these claims, arguing that Emanuel (2024) examined the flow curvature in the lower troposphere (850-OWZ proxy) rather than tracked TCs. Since the proxy may identify many atmospheric circulations that are not TCs, this could lead to trends that reflect a broader class of circulations rather than TCs alone. These conflicting findings underscore the substantial uncertainty in long-term TC frequency estimates from reanalyses, driven by changes in availability of observations, assimilation techniques, and the tracking algorithms used to identify TCs in reanalyses (Aarons et al., 2021; Bourdin et al., 2022; Hersbach et al., 2020).

Here, we revisit global and regional TC frequency trends over the past century by comparing multiple reanalyses. We analyze TC counts from two TC tracking methods to assess the sensitivity of results to the choice of tracking scheme. We also compare the trends in the environmental fields associated with TCs in 20CRv3 and 20CRv2c.

2. Data and Methods

We use TC track data for different reanalysis data sets from the Huracán Project (see https://research.reading.ac.uk/huracan/about-huracan/project-overview/). These TC tracks are based on the TRACK algorithm (Hodges et al., 2017). An additional data set derived using the Okubo–Weiss–Zeta (OWZ) algorithm (Tory et al., 2013) is considered to test the robustness to tracking method. Large-scale environmental fields from two reanalyses are also analyzed to assess the physical consistency of the detected TC frequency changes.

2.1. Best-Track Data Set

The International Best Track Archive for Climate Stewardship version 4 (IBTrACSv4; Knapp et al., 2010) with data from the National Hurricane Center (NHC) or the Joint Typhoon Warning Center (JTWC) are used as the observational reference. We consider IBTrACS TC counts during various periods, noting that substantial data quality issues remain especially before the satellite era (Klotzbach et al., 2022; Knutson et al., 2019; Vecchi & Knutson, 2008). We only consider observed TCs that reach at least tropical storm intensity (>34 kt) in our analysis.

2.2. Reanalysis Data Sets

TC track data available through the Huracán Project are obtained from four long-term reanalysis products (Table S1 in Supporting Information S1). Two are from the NOAA 20th Century Reanalysis project: version 3 (20CRv3, 1806–2015; L. C. Slivinski et al., 2019) and 2c (20CRv2c, 1831–2014; Compo et al., 2011), and two are from the European Center for Medium Range Forecasts (ECMWF): the Atmospheric Reanalysis of the 20th Century (ERA-20C, 1900–2010; Poli et al., 2016) and the Coupled Reanalysis of the 20th Century (CERA-20C, 1901–2010; Laloyaux et al., 2018). Each reanalysis spans over 100 years and avoids major artificial trends associated with evolving observing systems by assimilating only near-surface observations available throughout the record.

20CRv3 comprises 80 ensemble members. 20CRv2c is an earlier version of 20CRv3, with 56 ensemble members. 20CRv3 and v2c both assimilate only observations of surface pressure from multiple sources, including station measurements, marine observations, and, notably, TC pressure reports from IBTrACS (Compo et al., 2011; L. C. Slivinski et al., 2019). ERA-20C consists of a single ensemble, and assimilates surface pressure, marine winds as well as IBTrACS pressure reports (Poli et al., 2016). CERA-20C uses the same observations as ERA-20C but employs a coupled atmosphere-ocean model and includes 10 ensemble members (Laloyaux et al., 2018).

Our analysis focuses primarily on 20CRv3, for which the TRACK algorithm (Hodges et al., 2017) is applied to all 80 ensemble members, with comparisons to the other three reanalyses in which TRACK is applied to all available

ensemble members to assess the robustness of the reanalysis-based TC frequency trends. For large-scale environmental analysis, we directly use the 20CRv2c and 20CRv3 ensemble mean.

2.3. TC Tracking Algorithms

Given the sensitivity of TC counts to algorithm choice (e.g., Bourdin et al., 2022), we complement our analysis with 20CRv2c TC tracks derived using the Okubo–Weiss–Zeta (OWZ) algorithm (Tory et al., 2013). Both TRACK and OWZ rely on dynamics-based variables but differ in their detection philosophy: TRACK identifies TC-like vortices by tracking relative vorticity maxima on isobaric surfaces, whereas OWZ detects systems based on the OWZ parameter, emphasizing low-level vorticity and curvature thresholds (Bourdin et al., 2022).

2.4. LMI Thresholds and Analysis Definitions

We apply an intensity-based threshold criteria to the reanalysis-based TC tracks to exclude weak systems, based on their lifetime maximum intensity (LMI; maximum wind speed reached by a TC during its lifetime). Specifically, we use LMI thresholds of 15, 25, and 35-kt to examine the sensitivity of the TC frequency trends to these thresholds.

We explore long-term change in annual TC numbers at global and regional scales. Trend analyses focus on three main periods: 1850–2015, 1900–2015, and 1950–2015. The longest period begins at the pre-industrial baseline (1850–1900) to capture the full TC record derived from 20CR. By contrast, the 1900–2015 period allows comparison among reanalyses with overlapping coverage (Section 3.2), while 1950–2015 trends represent an era of more TC observations. Linear trends are evaluated using a two-sided t test, accounting for autocorrelation effects, and are considered significant with a p-value threshold of 0.05.

The annual number of TCs (NTC) refers to the total number of TCs forming during 12 months. The TC seasons are defined as January to December in the Northern Hemisphere, and July to June in the Southern Hemisphere, in order to take into account the peak TC season in each hemisphere. The TC basins are defined within the tropics (40°S–40°N) in each hemisphere: North Indian Ocean (NI), 0°E–90°E; Western North Pacific (WNP), 90°-E–180°E; Eastern North Pacific (ENP), 180°E to the west coast of America; North Atlantic (NATL), from the east coast of America to the 0°; South Indian Ocean (SI), 0°E–90°E; Australian Region (AUS), 90°E–170°E and South Pacific (SP), 170°E–240°E.

2.5. Environmental Fields

We also examined large-scale climate variables that are known to be closely related with TC genesis and have been widely used to understand changes in TC frequency. These include sea surface temperature (SST), mean sea level pressure (MSLP), vertical wind shear (VWS), column relative humidity (CRH), potential intensity (PI) (Bister & Emanuel, 2002), and a tropical cyclone genesis index (TCGI). The specific TCGI used here is based on PI, VWS, CRH and absolute vorticity at 850 hPa (Camargo et al., 2014, 2025; Tippett et al., 2011). We computed the changes in these variables from a pre-industrial baseline (1851–1900) for both 20CRv2c and 20CRv3 to evaluate consistency between versions and with TC frequency trends.

3. Results

3.1. TC Frequency Trends in 20CRv3

The TC frequency in the 20CRv3 data set and an LMI threshold of 15 kt shows a clear downward trend in global and hemispheric annual TC frequency over the century-scale 1900–2015 period, in contrast to an upward trend during 1850–1900 (Figure 1a; Figure S1 in Supporting Information S1). A similar NTC trend pattern is also evident in the NATL and WNP, as well as in most other basins except the NI and SI (Figure 1; Figure S1 in Supporting Information S1 top row). The results are mostly consistent with the findings of Chand et al. (2022), who used the earlier 20CRv2c with OWZ tracking algorithm, with the exception of the upward trend being weaker and the WNP showing a slight downward trend.

However, increasing the LMI threshold to 25 and 35 kt reverses the sign of the century-scale trend over 1900–2015, yielding increasing global-scale and basin-wide annual TC frequencies (Figure 1; Figure S1 in Supporting Information S1, middle and bottom rows). For example, the global trends over 1900–2015 shift from

19448007, 2026, 14, Downloaded from https://agupubs.onlinelibrary.wiley.com/doi/10.1029/2026GL122083 by NICE, National Institute for Health and Care Excellence, Wiley Online Library on [16/07/2026]. See the Terms and Conditions (https://onlinelibrary.wiley.com/terms-and-conditions) on Wiley Online Library for rules of use; OA articles are governed by the applicable Creative Commons License

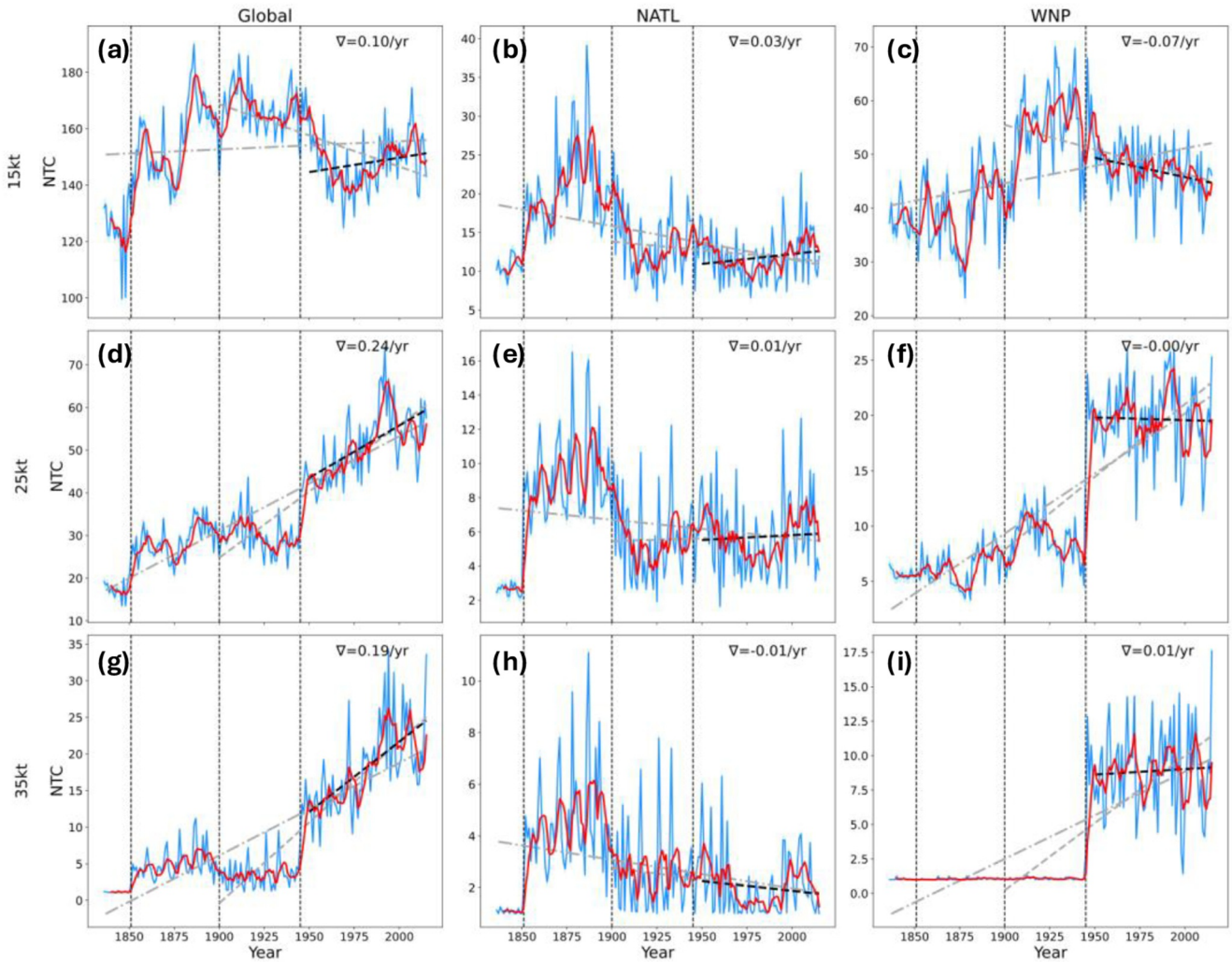

Figure 1. Time series of the 20CRv3 TC counts globally, in the NATL, and in the WNP from 1850 to 2015 with an increasing LMI threshold: TCs with LMI ≥15 kt, LMI ≥25 kt, and LMI ≥35 kt. Included is NTC (blue), a 5-year running mean (red), and trends post-1836, 1900, and 1950 (dashed lines with associated gradient (∇)). Dashed vertical lines indicate years 1850, 1900, and 1945.

−0.22 to +0.31, and +0.22 TCs per year as the LMI threshold increases from 15 to 25 and 35 kt, all of which are statistically significant (Table S2 in Supporting Information S1).

The reversal of the century-scale TC number trend with increasing LMI threshold reflects a discontinuity in the representation of slightly more intense storms in 20CRv3. As shown in Figure 1; Figure S1 in Supporting Information S1 (middle and bottom rows), higher LMI thresholds (≥25 kt) show pronounced step increases in the NTC around 1945. At the 25 kt threshold, global NTC exhibits a notable increase of about 20 TCs, compared to the earlier period (Figure 1d). At LMI ≥ 35 kt global TC counts are very low (approximately 5 TCs until around 1945, after which they rise sharply). The WNP contributes substantially to the step increase around 1945 (Figures 1f and 1i), which largely explains the upward shift in the global trends at the same time and thresholds (Figures 1d and 1g). Also contributing to this step increase, SH basins show a similar sensitivity to the LMI threshold, with discontinuities around (SI) or after (SP, AUS) 1945 (Figure S1 in Supporting Information S1).

This step increase is closely associated with the historical expansion of TC observations. IBTrACS data availability starts in 1851 for the NATL (Landsea & Franklin, 2013) and in 1945 for the WNP (Chu et al., 2002), and both records were subsequently assimilated into 20CRv3 (L. C. Slivinski et al., 2019). Consequently, the abrupt increase of 20 TCs in the global annual mean after 1945 likely reflects the improved detection and reporting of TCs after World War II (e.g., Emanuel, 2018), rather than a physical change in TC activity. In addition, evidence

19448007, 2026, 14, Downloaded from https://agupubs.onlinelibrary.wiley.com/doi/10.1029/2026GL122083 by NICE, National Institute for Health and Care Excellence, Wiley Online Library on [16/07/2026]. See the Terms and Conditions (https://onlinelibrary.wiley.com/terms-and-conditions) on Wiley Online Library for rules of use; OA articles are governed by the applicable Creative Commons License

19448007, 2026, 14, Downloaded from https://agupubs.onlinelibrary.wiley.com/doi/10.1029/2026GL122083 by NICE, National Institute for Health and Care Excellence, Wiley Online Library on [16/07/2026]. See the Terms and Conditions (https://onlinelibrary.wiley.com/terms-and-conditions) on Wiley Online Library for rules of use; OA articles are governed by the applicable Creative Commons License

from the LMI analysis suggests that the 1900–2015 decreasing trend—if real—mainly arises from weaker storms generated within the reanalysis. This trend may reflect a genuine climate signal in weak TC-like vortices or arise from changes in the density of assimilated observations, as suggested by Emanuel (2024).

Storms with an LMI between 15 and 25 kt, representing weak TCs, exhibit a significant downward trend (Figure S2 in Supporting Information S1). The ensemble spread of NTC likewise declines over time (Figure S3 in Supporting Information S1), indicating increased agreement among ensemble members as the number of assimilated surface pressure observations increases (Figure S4 in Supporting Information S1). Together, these results support the interpretation that increased assimilation of conventional observations suppresses spurious or "rogue" TCs that do not exist in nature but can arise in reanalyses under sparse observational constraints (Emanuel, 2024). This evidence suggests that the observed decline in the number of weak TCs could potentially be primarily driven by the increasing availability of conventional observations, rather than reflecting a physically meaningful change in NTC. In addition, we examine TC duration defined as the time a storm spends at or above each intensity threshold. For all storms with LMI $\geq$ 15 kt, the duration generally decreases over 1900–2015, whereas for stronger storms (LMI $\geq$ 25 and 35 kt; Figure S5 in Supporting Information S1), duration tends to increase or remain roughly unchanged, showing a reversal in TC duration trends as the LMI threshold increases. This behavior is consistent with the sensitivity of TC counts to LMI thresholds (Figure 1) and suggests that weak vortices are suppressed by the increase in observations.

3.2. Intercomparison of TC Frequency Trends Across Reanalyses and Tracking Methods

To assess the long-term trends of NTC across different data sets, we extend the analysis to other reanalyses, namely 20CRv2c, ERA-20C, and CERA-20C (Figure 2). As ERA-20C and CERA-20C begin in 1900, the comparison is limited to the 20th century. First, the total number of identified TCs varies across data sets, with ERA-20C yielding the fewest and 20CRv2c the most globally (see also Table S3 in Supporting Information S1). Second, both IBTrACS and 20CRv3 show a clear step increase around 1945, especially for global and WNP TCs as noted above, whereas 20CRv2c, ERA-20C, and CERA-20C display only moderate changes. Notably, the four reanalyses disagree substantially before 1950 but converge afterward, showing similar variability and no evident trends, indicating improved consistency during the modern observational era (Figure 2; Figure S6 in Supporting Information S1). Figure S7 in Supporting Information S1 also demonstrates progressively stronger correlations among reanalyses and with IBTrACS over time, from the early reanalysis period (post-1900) to the satellite era (post-1980), for both global and regional TCs, with the data over NATL consistently showing the highest agreement.

Overall, no single reanalysis appears more reliable for long-term TC trend analysis. All these reanalyses assimilate pressure data from the International Surface Pressure Databank, which integrates observations from land stations, marine platforms, and IBTrACS (Cram et al., 2015). However their TC representations differ due to variations in assimilation approaches and model configurations, particularly in how very low values of TC pressure data are handled (e.g., Laloyaux et al., 2018; L. C. Slivinski et al., 2019). For example, 20CRv3's higher-resolution forecast model enables more effective assimilation of very low central pressures of TCs. In contrast, 20CRv2c assimilates TC pressure data but assigns larger observational errors to stabilize assimilation (L. C. Slivinski et al., 2019), and CERA-20C and ERA-20C often reject very low pressure data values during quality control (Laloyaux et al., 2018). Consequently, the influence of IBTrACS and the associated step increase in TC frequency (Figures 1 and 2) is most evident in 20CRv3 than in the other reanalyses, while the influence of assimilation of IBTrACS on ERA-20C and CERA-20C is not straightforward.

In addition, the role of resolution in these reanalyses (Table S1 in Supporting Information S1) has an important impact on TC maximum intensity, but while the mean number of TCs tend to increase with resolution, this is not a linear relationship, as models with the same resolution can have very different number of global NTC (Camargo et al., 2020, 2025; Roberts et al., 2020). Because our LMI thresholds are very low, they are not filtering the intense storms most sensitive to resolution, so we do not expect the different resolutions (e.g., 20CRv3's higher resolution) to significantly impact these NTC trends. Beyond the direct effects of data assimilation, the increasing number of surface observations after around 1945 likely improved TC detectability in all reanalyses. This may partly explain the upward trends seen in ERA-20C, as well as the increasing agreement among reanalyses and with IBTrACS after 1950 (Figure 2; Figures S6 and S7 in Supporting Information S1).

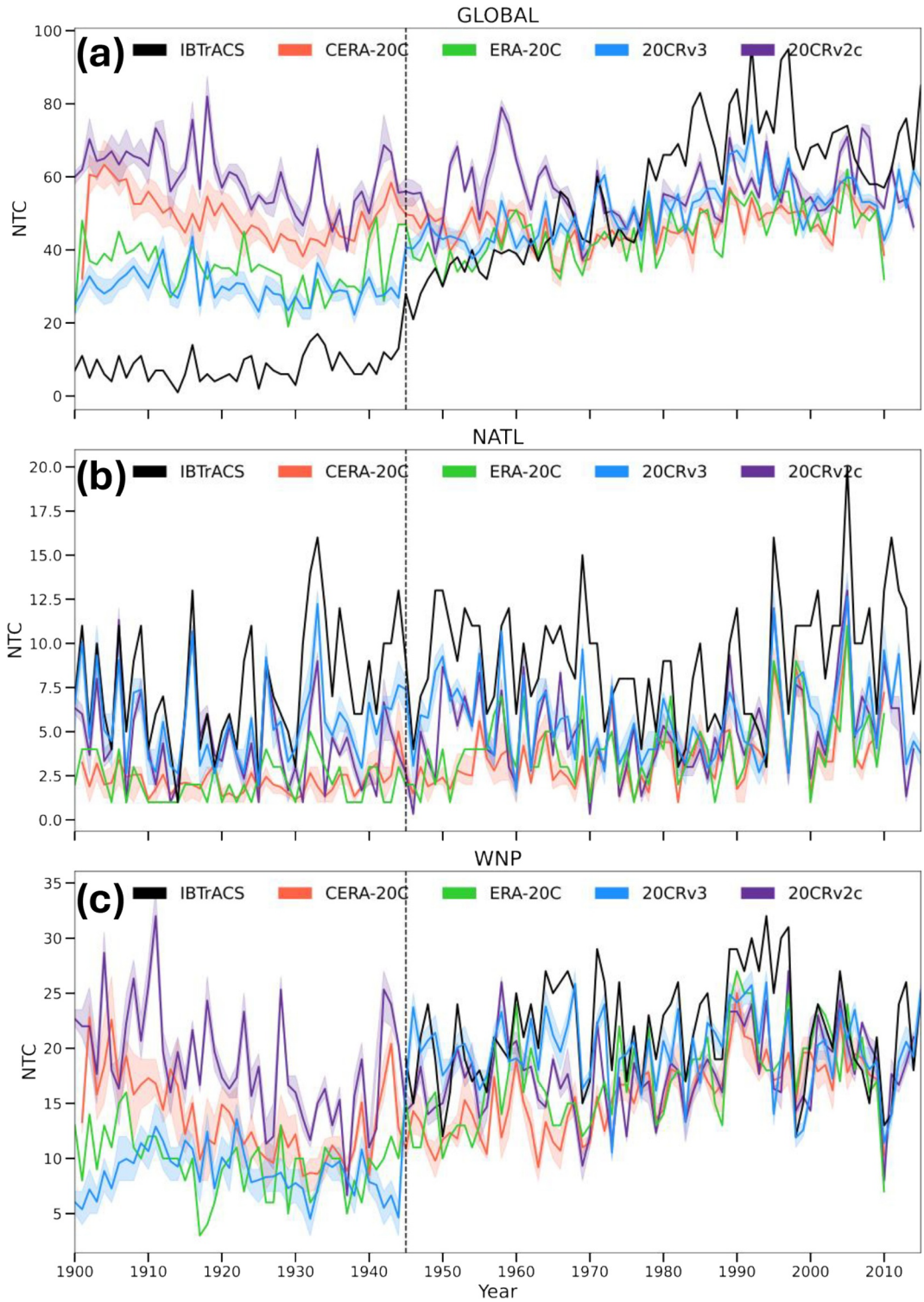

Figure 2. Time series of TC counts in IBTrACS (black), CERA-20C (orange), ERA-20C (green), 20CRv3 (blue), and 20CRv2c (purple): (a) global, (b) NATL, and (c) WNP basins over 1900–2015. Each reanalysis has a LMI ≥25 kt threshold, and IBTrACS has a LMI ≥35 kt threshold. Shading corresponds to the NTC ensemble spread at a 95% confidence interval for reanalyses with more than 1 ensemble member.

19448007, 2026, 14, Downloaded from https://agupubs.onlinelibrary.wiley.com/doi/10.1029/2026GL122083 by NICE, National Institute for Health and Care Excellence, Wiley Online Library on [16/07/2026]. See the Terms and Conditions (https://onlinelibrary.wiley.com/terms-and-conditions) on Wiley Online Library for rules of use; OA articles are governed by the applicable Creative Commons License

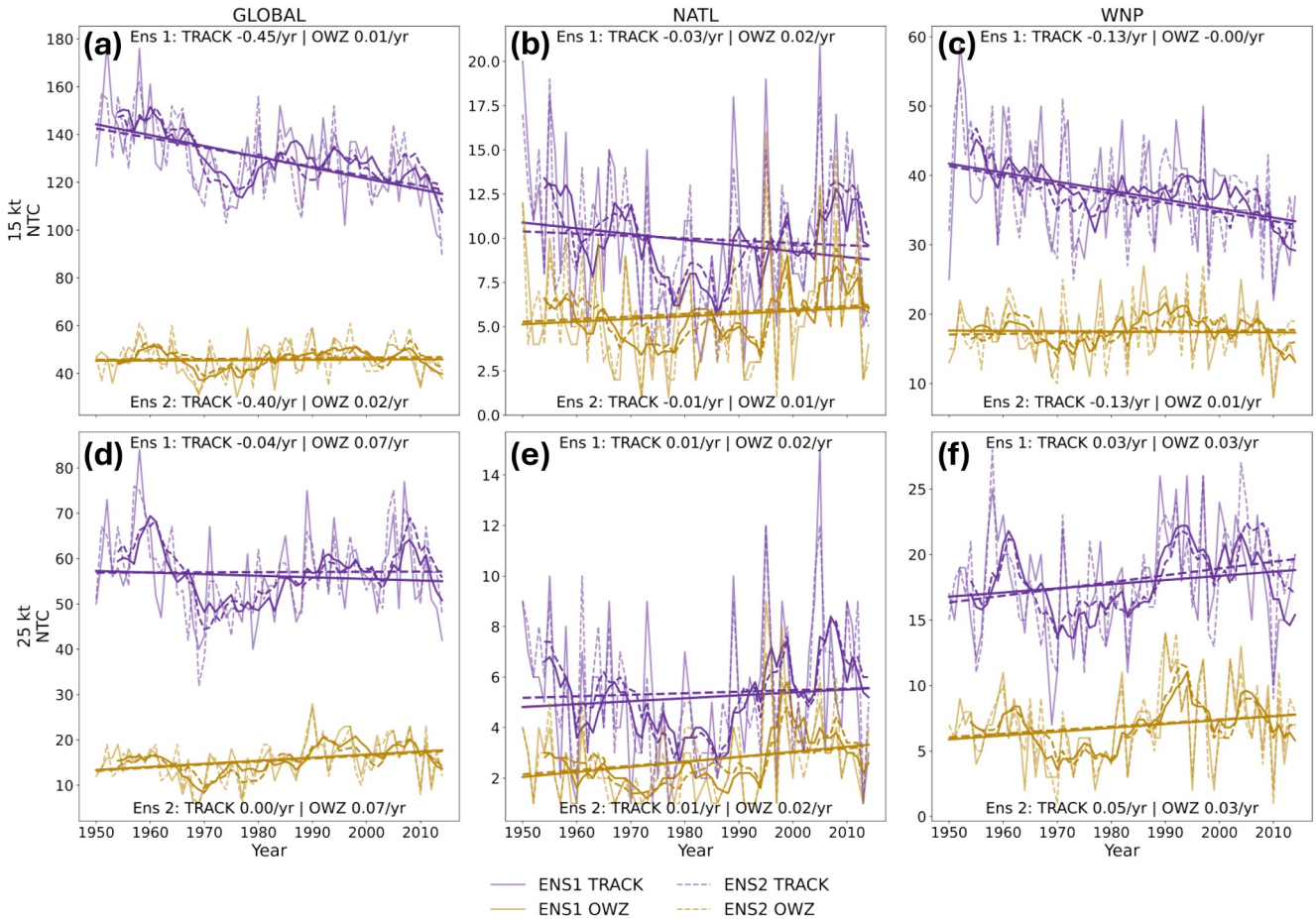

Figure 3. NTC time series for ensembles 1 and 2 20CRv2c based on TRACK (purple) and OWZ (gold) globally and for the NATL and WNP basins from 1950 to 2014 with LMI ≥15 kt (top panels) and ≥25 kt (bottom panels) thresholds. Ensemble one is shown in solid lines, ensemble 2 in dashed lines.

To assess the sensitivity of TC frequency trends to the choice of tracking algorithm, we compare two 20CRv2c ensemble members for which both TRACK and OWZ high frequency data variables are available. We focus on the 1950–2014 period, which represents a more consistent modern observational era and thus helps minimize the influence of large data uncertainties on the algorithm evaluation. As shown in Figure 3; Table S4 in Supporting Information S1, TRACK generally detects more TCs than OWZ (approximately 40, 3, and 10 more globally, in the NATL, and WNP, respectively, at 25 kt), as discussed in Bourdin et al. (2022). Despite these differences in absolute counts, the NTC trends exhibit a qualitatively similar sensitivity to the choice of LMI threshold, shifting from negative or near-zero trends to more positive values as the threshold increases, indicating that TC frequency trends are determined by the reanalysis and not by the choice of tracking algorithm (Figure 3; Figure S9 and Table S4 in Supporting Information S1). However, since both TRACK and OWZ tend to include weaker storms, this finding may not extend to more restrictive tracking algorithms.

Figure S8 in Supporting Information S1 extends this comparison to 20CRv3, although the setups are not directly comparable: in 20CRv2c, two individual ensemble members are analyzed, whereas in 20CRv3, TRACK represents the mean of 80 ensemble members and OWZ is derived from the ensemble-mean environmental state, based on data from (Ye et al., 2024). Notwithstanding these methodological differences, the NTC trends derived from TRACK and OWZ remain generally consistent in both sign and magnitude. In addition, Figure S9 in Supporting Information S1 illustrates that the 1900–2015 trend reverses from negative to positive when the LMI threshold increases from 15 to 25 kt in both 20CRv2c + OWZ and 20CRv2c + TRACK, confirming that TC frequency trends in both 20CRv3 and v2c are highly sensitive to the chosen LMI threshold but largely insensitive to the tracking algorithm.

19448007, 2026, 14, Downloaded from https://agupubs.onlinelibrary.wiley.com/doi/10.1029/2026GL122083 by NICE, National Institute for Health and Care Excellence, Wiley Online Library on [16/07/2026]. See the Terms and Conditions (https://onlinelibrary.wiley.com/terms-and-conditions) on Wiley Online Library for rules of use; OA articles are governed by the applicable Creative Commons License

10.1029/2026GL122083

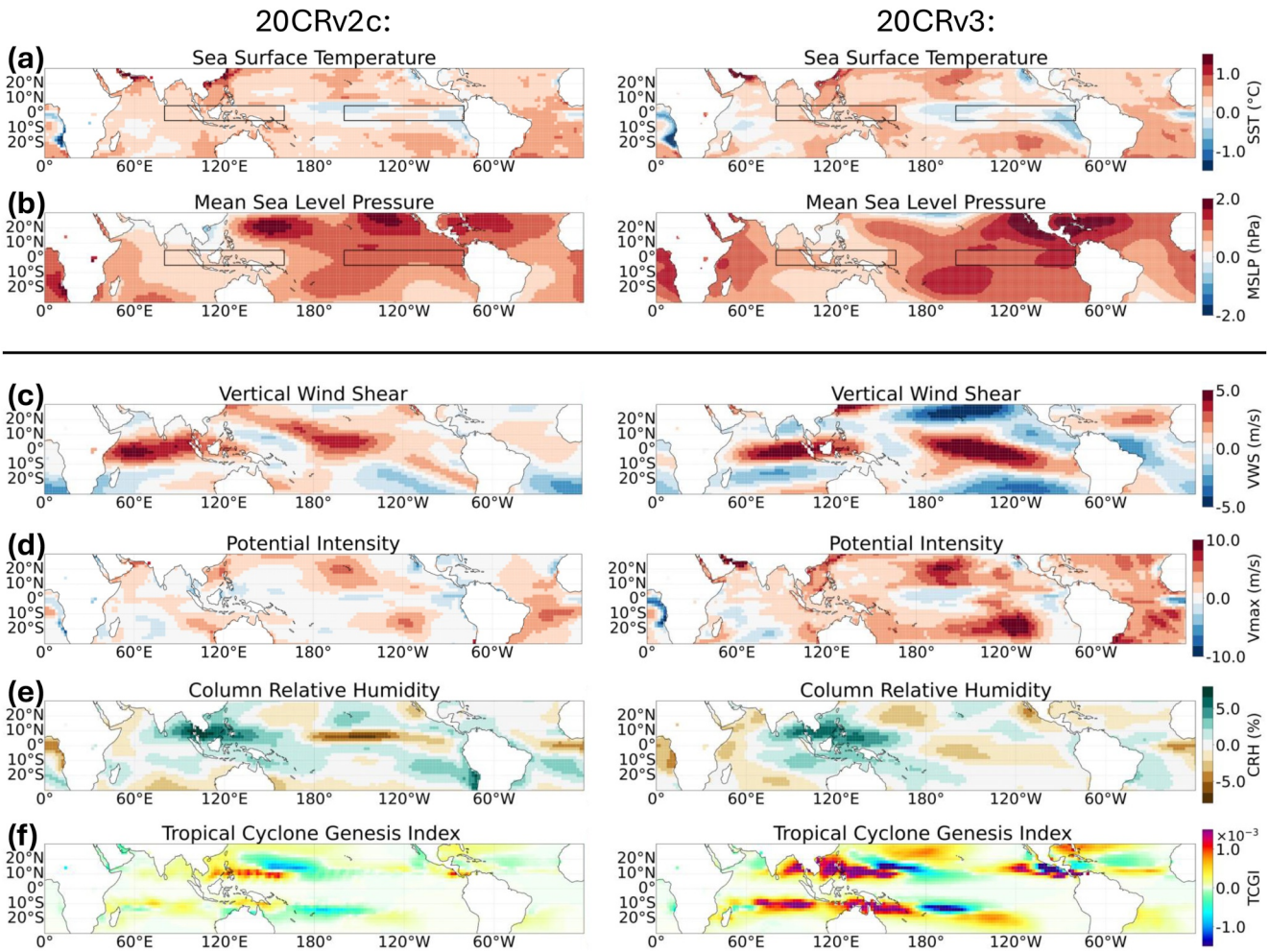

Figure 4. Changes in (a) sea surface temperature, (b) mean sea level pressure, (c) vertical wind shear, (d) potential intensity, (e) column relative humidity, and (f) tropical cyclone genesis index between the historical period (1951–2010) and the preindustrial period 1851–1900) in 20CRv2c (left) and 20CRv3 (right).

3.3. Large-Scale Environmental Fields

Here we examine changes (present: 1951–2010) from the pre-industrial baseline (1851–1900) in the large-scale environmental fields that influence TC frequency, to assess whether the TC trends identified in 20CRv3 and 20CRv2c can be linked to changes in their background environments. Figure 4a shows widespread tropical SST warming, accompanied by limited warming or even cooling in the central to eastern equatorial Pacific, resulting in an enhanced zonal SST gradient across the equatorial Pacific (Figure S10a in Supporting Information S1) (e.g., Seager et al., 2019; Seager et al., 2022). The associated enhancement of the zonal MSLP gradient (Figure 4b; Figure S10b in Supporting Information S1) is consistent with this strengthened SST gradient and indicates an intensifying Walker circulation. At the global scale, changes in the Walker circulation reflect large-scale tropical overturning and largely determine the mean vertical motion (e.g., Held & Zhao, 2011). A strengthening of the Walker circulation manifests as increased upward mass flux in the ascending branches, where deep tropical convection is most active, thereby contributing to a more overall favorable large-scale environment for TC formation (e.g., Vecchi & Soden, 2007). At the regional scale, particularly over the western Pacific warm pool, a strengthened Walker circulation enhances ascent over this primary TC genesis region, increasing mid-level humidity and reducing saturation deficit, thereby favoring TC formation. This interpretation aligns with Chand et al. (2022), despite the attributed the decline in TC frequency in 20CRv2c to a weakening Walker circulation inferred from a different MSLP data set (Kaplan et al., 2000). Nevertheless, the Walker circulation represents only one aspect of the large-scale environment, and TC activity is influenced by multiple environmental factors (e.g., Sobel et al., 2021; Vecchi et al., 2019).

19448007, 2026, 14, Downloaded from https://agupubs.onlinelibrary.wiley.com/doi/10.1029/2026GL122083 by NICE, National Institute for Health and Care Excellence, Wiley Online Library on [16/07/2026]. See the Terms and Conditions (https://onlinelibrary.wiley.com/terms-and-conditions) on Wiley Online Library for rules of use; OA articles are governed by the applicable Creative Commons License

19448007, 2026, 14, Downloaded from https://agupubs.onlinelibrary.wiley.com/doi/10.1029/2026GL122083 by NICE, National Institute for Health and Care Excellence, Wiley Online Library on [16/07/2026]. See the Terms and Conditions (https://onlinelibrary.wiley.com/terms-and-conditions) on Wiley Online Library for rules of use; OA articles are governed by the applicable Creative Commons License

However, beyond the large-scale circulation metrics, we find no coherent or substantial changes in individual TC-relevant environmental fields, including vertical wind shear (Figure 4c; Figure S10c in Supporting Information S1), potential intensity (Figure 4d; Figure S10d in Supporting Information S1), column relative humidity (Figure 4e; Figure S10e in Supporting Information S1), or the TC genesis index (Figure 4f; Figure S10f in Supporting Information S1), that would be capable of explaining the pronounced step like increase in TC frequency observed after 1945 (Figure 1). We also directly examined TC genesis density (Figure S11 in Supporting Information S1) which shows a widespread increase in TC occurrence across basins, consistent with the results shown in Figure 1; Figure S1 in Supporting Information S1, but again revealed discrepancies between the two versions, namely in the Central and South Pacific, consistent with Figure 4. This suggests that the step increase after 1945 is unlikely to be a product of changes within the large-scale environmental fields, but rather it is probably related to changes in availability in the observational pressure data assimilated.

Crucially, the comparison between 20CRv2c and 20CRv3 environmental fields reveals substantial discrepancies in both the spatial patterns of the changes in large-scale environments, and their magnitude (Figure 4). For example, the magnitude of changes between the preindustrial and historical periods is generally larger in 20CRv3, with particularly pronounced differences in the eastern North and South Pacific (Figure 4f). In addition, the tropical mean column relative humidity even exhibits opposite trends in 20CRv2c and 20CRv3 (Figure S10e in Supporting Information S1). These inconsistencies indicate that even the sign and amplitude of large scale environmental trends are not robust across 20CR versions. Such uncertainty undermines confidence in attributing long term TC frequency trends inferred from these reanalyses to physically meaningful changes in the background environment.

4. Conclusion

Based on the 20CRv3 reanalysis, which provides a best-guess reconstruction of atmospheric conditions since the 1850s, we assessed historical long-term trends of TC frequency. Our results show that TC frequency trends are highly sensitive to the LMI threshold applied. For LMI threshold $\geq$15 kt, global and regional TC frequency declines significantly from 1900 to 2015. However, raising the threshold to 25 or 35 kt, thereby excluding weaker systems, shifts the trend to more positive values, yielding increases of TC frequency at both global and regional scales. We also identify discontinuities in TC frequency around 1945, coinciding with the post–World War II expansion of systematic observations in the NATL and WNP. This result clearly shows that 20CRv3 inherits TC data density and quality issues from IBTrACS. Consequently, TCs detected in 20CRv3 reanalyses should not be used to infer long-term trends.

The detected TC frequency trends in 20CR and their sensitivity to LMI thresholds are robust across different tracking algorithms but vary with reanalysis data sets. Because all reanalyses studied here assimilate the International Surface Pressure Databank, which includes pressure reports from IBTrACS, they inevitably inherit data issues from best-track data sets, though in different ways depending on assimilation schemes and model design. In addition, our analysis of environmental fields reveals stark discrepancies between 20CRv2c and 20CRv3, further underscoring that long-term TC frequency trends derived from the 20CR data sets are not robust.

Historical reanalyses nevertheless remain valuable for studying extremes, particularly where satellite-era records are too short. Midlatitude storms, heat waves, and cold-air outbreaks are often well represented in regions with dense observations (Brönnimann & Luterbacher, 2012; Donat et al., 2013; Messori et al., 2016). By contrast, tropical cyclones are more difficult to model—requiring high resolution—and remain poorly constrained by observations. A key aspect of using reanalyses is therefore to properly account for their uncertainties (e.g., Parker, 2016). Despite the issues we identify for TCs in 20CRv2c and 20CRv3, it remains challenging to detect true changes in TC frequency while disentangling artifacts in reanalysis trends that arise from the combined influence of models and observations.

Conflict of Interest

The authors declare no conflicts of interest relevant to this study.

Availability Statement

Twentyth Century Reanalysis data sets 20CRv3 (L. C. Slivinski et al., 2019) and 20CRv2c (Compo et al., 2011) are provided by the NOAA PSL, Boulder, Colorado, USA, from their website at https://psl.noaa.gov. European Centre for Medium-Range Weather Forecasts (ECMWF) data sets ERA-20C (Poli et al., 2016) and CERA-20C (Laloyaux et al., 2018) are available at https://apps.ecmwf.int/datasets/. NOAA's International Best Track Archive for Climate Stewardship (IBTrACS (Knapp et al., 2010);) data, last accessed on 28 May 2024, is available at https://www.ncei.noaa.gov/products/international-best-track-archive. Huracán tropical cyclone tracks are available at https://research.reading.ac.uk/huracan/science/data/. OWZ track data for two ensembles of 20CRv2c are available at https://github.com/savinchand/20CRv2-TC-Tracks. OWZ track data for 20CRv3 shown in Figure S6 of Supporting Information S1 is available at https://doi.org/10.5281/zenodo.14411917 (Ye et al., 2024).

Acknowledgments
We thank Kerry Emanuel (MIT) for valuable comments to improve our manuscript. Kailey Jones was partially supported by NOAA MAPP NA21OAR4310345. Jing-Yi Zhuo was partially supported by NSF AGS-22-17618, DOE SC0023333 and the Heising-Simons Foundation. Suzana Camargo was partially supported by NOAA MAPP NA21OAR4310345 and NSF AGS-2244918.

References

Aarons, Z. S., Camargo, S. J., Strong, J. D. O., & Murakami, H. (2021). Tropical cyclone characteristics in the MERRA-2 reanalysis and AMIP simulations. *Earth and Space Science*, *8*(3), e2020EA001415. https://doi.org/10.1029/2020EA001415

Bister, M., & Emanuel, K. A. (2002). Low frequency variability of tropical cyclone potential intensity 1. Interannual to interdecadal variability. *Journal of Geophysical Research*, *107*(D24), 4801. https://doi.org/10.1029/2001jd000776

Bourdin, S., Fromang, S., Dulac, W., Cattiaux, J., & Chauvin, F. (2022). Intercomparison of four algorithms for detecting tropical cyclones using ERA5. *Geoscientific Model Development*, *15*(17), 6759–6786. https://doi.org/10.5194/gmd-15-6759-2022

Brönnimann, S., & Luterbacher, J. (2012). Weather and climate extremes during the past 100 years. *Meteorologische Zeitschrift*, *21*(1), 9–11. https://doi.org/10.1127/0941-2948/2012/0525

Camargo, S. J., Giulivi, C. F., Sobel, A. H., Wing, A. A., Kim, D., Moon, Y., et al. (2020). Characteristics of model tropical cyclone climatology and the large-scale environment. *Journal of Climate*, *33*(11), 4463–4487. https://doi.org/10.1175/jcli-d-19-0500.1

Camargo, S. J., Murakami, H., Bloemendaal, N., Chand, S. S., Deshpande, M. S., Dominguez-Sarmiento, C., et al. (2023). An update on the influence of natural climate variability and anthropogenic climate change on tropical cyclones. *Tropical Cyclone Research and Review*, *12*(3), 216–239. https://doi.org/10.1016/j.tcrr.2023.10.001

Camargo, S. J., Tippett, M. K., Sobel, A. H., Lee, C.-Y., Fosu, B., & Hodges, K. I. (2025). Tropical cyclones and associated environmental fields in cmip6 models. *Journal of Climate*, *38*(15), 3877–3902. https://doi.org/10.1175/jcli-d-24-0629.1

Camargo, S. J., Tippett, M. K., Sobel, A. H., Vecchi, G. A., & Zhao, M. (2014). Testing the performance of tropical cyclone genesis indices in future climates using the HiRAM model. *Journal of Climate*, *27*(24), 9171–9196. https://doi.org/10.1175/JCLI-D-13-00505.1

Chand, S. S., Walsh, K. J. E., Camargo, S. J., Kossin, J. P., Tory, K. J., Wehner, M. F., et al. (2022). Declining tropical cyclone frequency under global warming. *Nature Climate Change*, *12*(7), 655–661. https://doi.org/10.1038/s41558-022-01388-4

Chand, S. S., Walsh, K. J. E., Camargo, S. J., Kossin, J. P., Tory, K. J., Wehner, M. F., et al. (2023). Reply to: Limitations of reanalyses for detecting tropical cyclone trends. *Nature Climate Change*, *14*(2), 146–147. https://doi.org/10.1038/s41558-023-01880-5

Chu, J.-H., Sampson, C. R., Levine, A. S., & Fukada, E. (2002). *The Joint Typhoon Warning Center tropical cyclone best-tracks, 1945–2000*. (Tech. Rep. No. Rep. NRL/MR/7540-02-16). Joint Typhoon Warning Center.

Compo, G. P., Whitaker, J. S., Sardeshmukh, P. D., Matsui, N., Allan, R. J., Yin, X., et al. (2011). The 20th century reanalysis project. *Quarterly Journal of the Royal Meteorological Society*, *137*(654), 1–28. https://doi.org/10.1002/qj.776

Cram, T. A., Compo, G. P., Yin, X., Allan, R. J., McColl, C., Vose, R. S., et al. (2015). The international surface pressure databank version 2. *Geoscience Data Journal*, *2*(1), 31–46. https://doi.org/10.1002/gdj3.25

Donat, M. G., Alexander, L. V., Yang, H., Durre, I., Vose, R., Dunn, R. J. H., et al. (2013). Updated analyses of temperature and precipitation extreme indices since the beginning of the 20th century: The hadex2 dataset. *Journal of Geophysical Research: Atmospheres*, *118*(5), 2098–2118. https://doi.org/10.1002/jgrd.50150

Emanuel, K. (2018). 100 years of progress in tropical cyclone research. *Meteorological Monographs*, *59*, 15.1–15.68. https://doi.org/10.1175/amsmonographs-d-18-0016.1

Emanuel, K. (2024). Limitations of reanalyses for detecting tropical cyclone trends. *Nature Climate Change*, *14*(2), 143–145. https://doi.org/10.1038/s41558-023-01879-y

Held, I. M., & Zhao, M. (2011). The response of tropical cyclone statistics to an increase in CO_2 with fixed sea surface temperatures. *Journal of Climate*, *24*(20), 5353–5364. https://doi.org/10.1175/jcli-d-11-00050.1

Hersbach, H., Bell, B., Berrisford, P., Hirahara, S., Horányi, A., Muñoz-Sabater, J., et al. (2020). The ERA5 global reanalysis. *Quarterly Journal of the Royal Meteorological Society*, *146*(730), 1999–2049. https://doi.org/10.1002/qj.3803

Hodges, K., Cobb, A., & Vidale, P. L. (2017). How well are tropical cyclones represented in reanalysis datasets? *Journal of Climate*, *30*(14), 5243–5264. https://doi.org/10.1175/jcli-d-16-0557.1

Kaplan, A., Kushnir, Y., & Cane, M. A. (2000). Reduced space optimal interpolation of historical marine sea level pressure: 1854–1992. *Journal of Climate*, *13*(16), 2987–3002. https://doi.org/10.1175/1520-0442(2000)013⟨2987:rsoioh⟩2.0.co;2

Klotzbach, P. J., Wood, K. M., Schreck, C. J., Bowen, S. G., Patricola, C. M., & Bell, M. M. (2022). Trends in global tropical cyclone activity: 1990–2021. *Geophysical Research Letters*, *49*(6), e2021GL095774. https://doi.org/10.1029/2021GL095774

Knapp, K. R., Kruk, M. C., Levinson, D. H., Diamond, H. J., & Neumann, C. J. (2010). The international best track archive for climate stewardship (IBTrACS): Unifying tropical cyclone data. *Bulletin of the American Meteorological Society*, *91*(3), 363–376. https://doi.org/10.1175/2009BAMS2755.1

Knutson, T., Camargo, S. J., Chan, J. C. L., Emanuel, K., Ho, C.-H., Kossin, J., et al. (2019). Tropical cyclones and climate change assessment: Part I: Detection and attribution. *Bulletin of the American Meteorological Society*, *100*(10), 1987–2007. https://doi.org/10.1175/bams-d-18-0189.1

Kossin, J. P., Knapp, K. R., Vimont, D. J., Murnane, R. J., & Harper, B. A. (2007). A globally consistent reanalysis of hurricane variability and trends. *Geophysical Research Letters*, *34*(4), L04815. https://doi.org/10.1029/2006GL028836

19448007, 2026, 14, Downloaded from https://agupubs.onlinelibrary.wiley.com/doi/10.1029/2026GL122083 by NICE, National Institute for Health and Care Excellence, Wiley Online Library on [16/07/2026]. See the Terms and Conditions (https://onlinelibrary.wiley.com/terms-and-conditions) on Wiley Online Library for rules of use; OA articles are governed by the applicable Creative Commons License

Kossin, J. P., Olander, T. L., & Knapp, K. R. (2013). Trend analysis with a new global record of tropical cyclone intensity. *Journal of Climate*, *26*(24), 9960–9976. https://doi.org/10.1175/jcli-d-13-00262.1

Laloyaux, P., De Boisseson, E., Balmaseda, M., Bidlot, J., Broennimann, S., Buizza, R., et al. (2018). CERA-20C: A coupled reanalysis of the 20th century. *Journal of Advances in Modeling Earth Systems*, *10*(5), 1172–1195. https://doi.org/10.1029/2018MS001273

Landsea, C. (2007). Counting Atlantic tropical cyclones back to 1900. *EOS Transactions of the American Geophysical Union*, *88*(18), 197–202. https://doi.org/10.1029/2007eo180001

Landsea, C. W., & Franklin, J. L. (2013). Atlantic hurricane database uncertainty and presentation of a new database format. *Monthly Weather Review*, *141*(10), 3576–3592. https://doi.org/10.1175/mwr-d-12-00254.1

Landsea, C. W., Vecchi, G. A., Bengtsson, L., & Knutson, T. R. (2010). Impact of duration thresholds on Atlantic tropical cyclone counts. *Journal of Climate*, *23*(10), 2508–2519. https://doi.org/10.1175/2009jcli3034.1

Messori, G., Caballero, R., & Gaetani, M. (2016). On cold spells in North America and storminess in western Europe. *Geophysical Research Letters*, *43*(12), 6620–6628. https://doi.org/10.1002/2016gl069392

Murakami, H., Delworth, T. L., Cooke, W. F., Zhao, M., Xiang, B., & Hsu, P.-C. (2020). Detected climatic change in global distribution of tropical cyclones. *Proceedings of the National Academy of Sciences*, *117*(20), 10706–10714. https://doi.org/10.1073/pnas.1922500117

Poli, P., Hersbach, H., Dee, D. P., Berrisford, P., Simmons, A. J., Vitart, F., et al. (2016). ERA-20C: An atmospheric reanalysis of the 20th century. *Journal of Climate*, *29*(11), 4083–4097. https://doi.org/10.1175/JCLI-D-15-0556.1

Roberts, M. J., Camp, J., Seddon, J., Vidale, P. L., Hodges, K., Vannière, B., et al. (2020). Projected future changes in tropical cyclones using the cmip6 highresmip multimodel ensemble. *Geophysical Research Letters*, *47*(14), e2020GL088662. https://doi.org/10.1029/2020gl088662

Seager, R., Cane, M., Henderson, N., Lee, D.-E., Abernathey, R., & Zhang, H. (2019). Strengthening tropical Pacific zonal sea surface temperature gradient consistent with rising greenhouse gases. *Nature Climate Change*, *9*(7), 517–522. https://doi.org/10.1038/s41558-019-0505-x

Seager, R., Henderson, N., & Cane, M. (2022). Persistent discrepancies between observed and modeled trends in the tropical Pacific Ocean. *Journal of Climate*, *35*(14), 4571–4584. https://doi.org/10.1175/jcli-d-21-0648.1

Slivinski, L., Compo, G., Whitaker, J., Sardeshmukh, P., Giese, B., McColl, C., et al. (2019). NOAA-CIRES-DOE 20th century reanalysis version 3. https://doi.org/10.5065/H93G-WS83

Slivinski, L. C. (2018). Historical reanalysis: What, how, and why? *Journal of Advances in Modeling Earth Systems*, *10*(8), 1736–1739. https://doi.org/10.1029/2018MS001434

Slivinski, L. C., Compo, G. P., Whitaker, J. S., Sardeshmukh, P. D., Giese, B. S., McColl, C., et al. (2019). Towards a more reliable historical reanalysis: Improvements for version 3 of the Twentieth Century Reanalysis system. *Quarterly Journal of the Royal Meteorological Society*, *145*(724), 2876–2908. https://doi.org/10.1002/qj.3598

Sobel, A. H., Wing, A. A., Camargo, S. J., Patricola, C. M., Vecchi, G. A., Lee, C., & Tippett, M. K. (2021). Tropical cyclone frequency. *Earth's Future*, *9*(12), e2021EF002275. https://doi.org/10.1029/2021ef002275

Tippett, M. K., Camargo, S. J., & Sobel, A. H. (2011). A poisson regression index for tropical cyclone genesis and the role of large-scale vorticity in genesis. *Journal of Climate*, *24*(9), 2335–2357. https://doi.org/10.1175/2010JCLI3811.1

Tory, K. J., Chand, S. S., Dare, R. A., & McBride, J. L. (2013). The development and assessment of a model-grid-and basin-independent tropical cyclone detection scheme. *Journal of Climate*, *26*(15), 5493–5507. https://doi.org/10.1175/JCLI-D-12-00510.1

Vecchi, G. A., Delworth, T. L., Murakami, H., Underwood, S. D., Wittenberg, A. T., Zeng, F., et al. (2019). Tropical cyclone sensitivities to CO_2 doubling: Roles of atmospheric resolution, synoptic variability and background climate changes. *Climate Dynamics*, *53*(9–10), 5999–6033. https://doi.org/10.1007/s00382-019-04913-y

Vecchi, G. A., & Knutson, T. R. (2008). On estimates of historical North Atlantic tropical cyclone activity. *Journal of Climate*, *21*(14), 3580–3600. https://doi.org/10.1175/2008jcli2178.1

Vecchi, G. A., Landsea, C., Zhang, W., Villarini, G., & Knutson, T. (2021). Changes in Atlantic major hurricane frequency since the late-19th century. *Nature Communications*, *12*(1), 4054. https://doi.org/10.1038/s41467-021-24268-5

Vecchi, G. A., & Soden, B. J. (2007). Increased tropical Atlantic wind shear in model projections of global warming. *Geophysical Research Letters*, *34*(8). https://doi.org/10.1029/2006gl028905

Ye, G., Leung, J., Wenjie, D., Jianjun, X., Weijing, L., Weihong, Q., et al. (2024). Reanalysis-based global tropical cyclone tracks dataset for the 20th century (rgtracks-20c). *Zenodo*. https://doi.org/10.5281/ZENODO.8410596

19448007, 2026, 14, Downloaded from https://agupubs.onlinelibrary.wiley.com/doi/10.1029/2026GL122083 by NICE, National Institute for Health and Care Excellence, Wiley Online Library on [16/07/2026]. See the Terms and Conditions (https://onlinelibrary.wiley.com/terms-and-conditions) on Wiley Online Library for rules of use; OA articles are governed by the applicable Creative Commons License